Supporting Information

Pursuit of Record Breaking Energy Barriers: A Study of Magnetic Axiality in Diamide Ligated Dy^{III} Single-Molecule Magnets

Katie L. M. Harriman,[a] Jonathan L. Brosmer,[b] Liviu Ungur,[,c,d] Paula L. Diaconescu,*[,b] and Muralee Murugesu*[,a]*

[a] Department of Chemistry and Biomolecular Sciences, and Centre for Catalysis Research and Innovation, University of Ottawa, Ottawa, Ontario K1N 6N5, Canada

[b] Department of Chemistry and Biochemistry, University of California, Los Angeles, California 90095, USA

[c] Theory of Nanomaterials Group and INPAC – Institute of Nanoscale Physics and Chemistry, Katholieke, Universiteit Leuven, Celestijnenlaan 200F, 3001 Leuven Belgium

[d] Theoretical Chemistry, Lund University, Getingevagen 60, 22241, Lund Sweden

*Corresponding Authors: L. Ungur (E-mail: Liviu.Ungur@chem.kuleuven.be); P. L. Diaconescu (E-mail: pld@chem.ucla.edu; Tel: +1 (310) 794 4809); M. Murugesu (E-mail: m.murugesu@uottawa.ca; Tel: +1 (613) 562 5800 ext 2733)

Contents

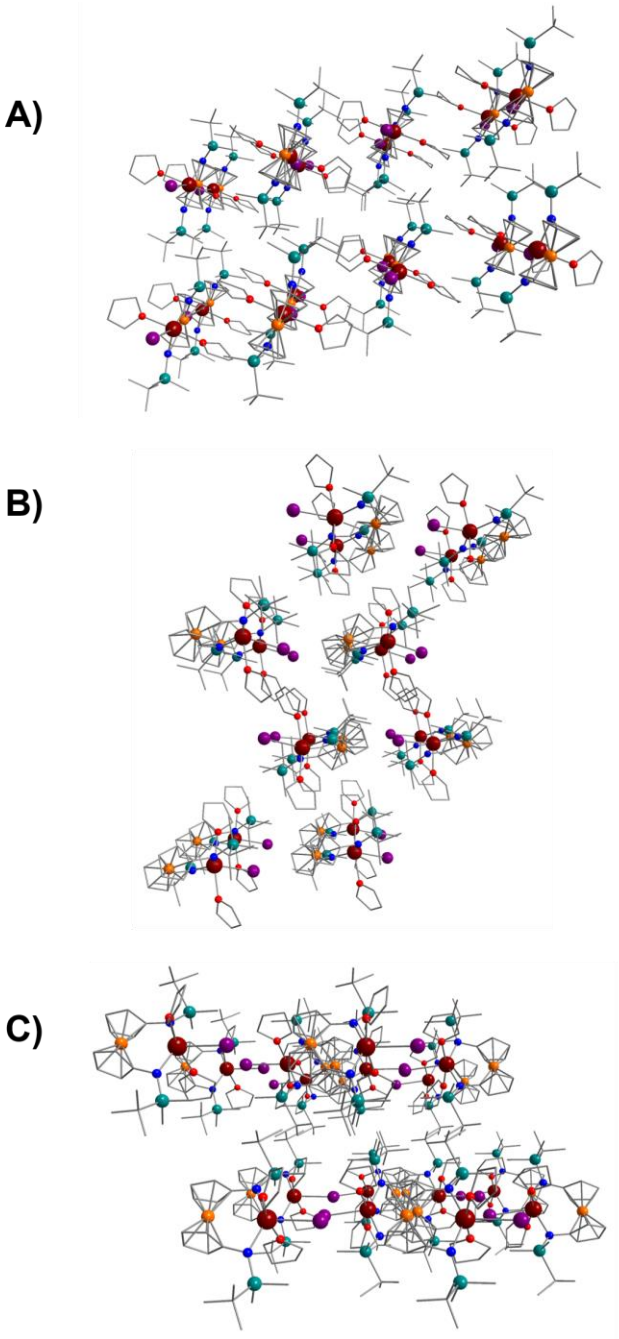

Figure S1. Crystallographic packing diagrams of (**NN^{TBS})DyI(THF)$_2$** (**1-Dy**): (a) along the *a*-axis, (b) along the *b*-axis, and (c) along the *c*-axis. Color code: Dy; dark red, Fe; orange, I; purple, N; royal blue, O; red, Si; teal, C; grey, hydrogen atoms have been omitted for clarity.

Table S1. SHAPE measurements of **1-Dy** relative to an ideal 5-vertex polyhedron shown. The best match is displayed in red.

SHAPE Code	Point Group	Description	1-Dy
PP-5	D_{5h}	Pentagon	34.648
vOC-5	C_{4v}	Vacant octahedron (Johnson square pyramid)	7.187
TBPY-5	D_{3h}	Trigonal bipyramid	**1.004**
SPY-5	C_{4v}	Square pyramid	5.330
JTBPY-5	D_{3h}	Johnson trigonal bipyramid	4.762

Magnetic Property Measurements. The magnetic susceptibility measurements were obtained using a Quantum Design SQUID magnetometer MPMS-XL7 operating between 1.8 and 300 K for dc fields ranging from -7 to 7 T. Dc susceptibility measurements were performed on a polycrystalline sample (30 mg) of **1-Dy** sealed in a polyethylene membrane prepared under an inert atmosphere, and subjected to a field of 0 to 7 T. Ac susceptibility measurements were carried out under an oscillating field of 3.78 Oe and ac frequencies 0.1 to 1500 Hz and dc fields ranging from 0 to 1200 Oe. The magnetization data were collected at 100 K to check for ferromagnetic impurities that were absent in the sample. Diamagnetic corrections were applied for the sample holder and the inherent diamagnetism of the sample was estimated with the use of Pascals constants.

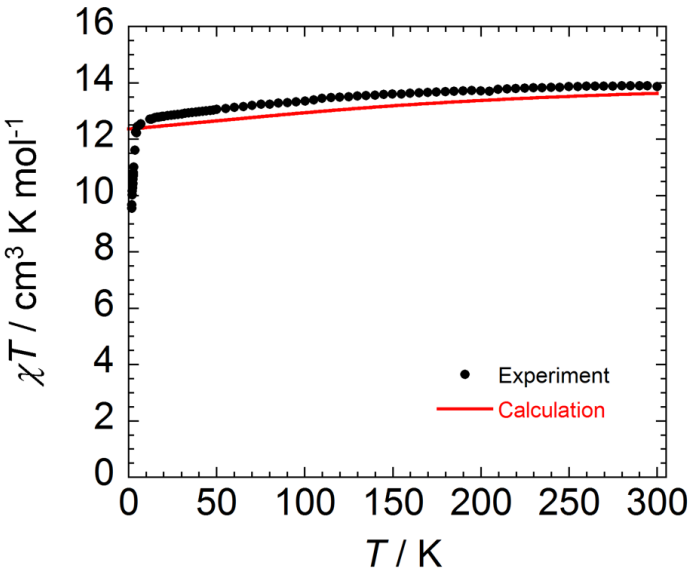

Figure S2. Temperature dependence of the χT product at 1 kOe for **1-Dy**, with χ being the molar magnetic susceptibility per molecule as defined by M/H. Experimental data is represented by black circles and *ab initio* calculated magnetic susceptibility depicted by the solid red line.

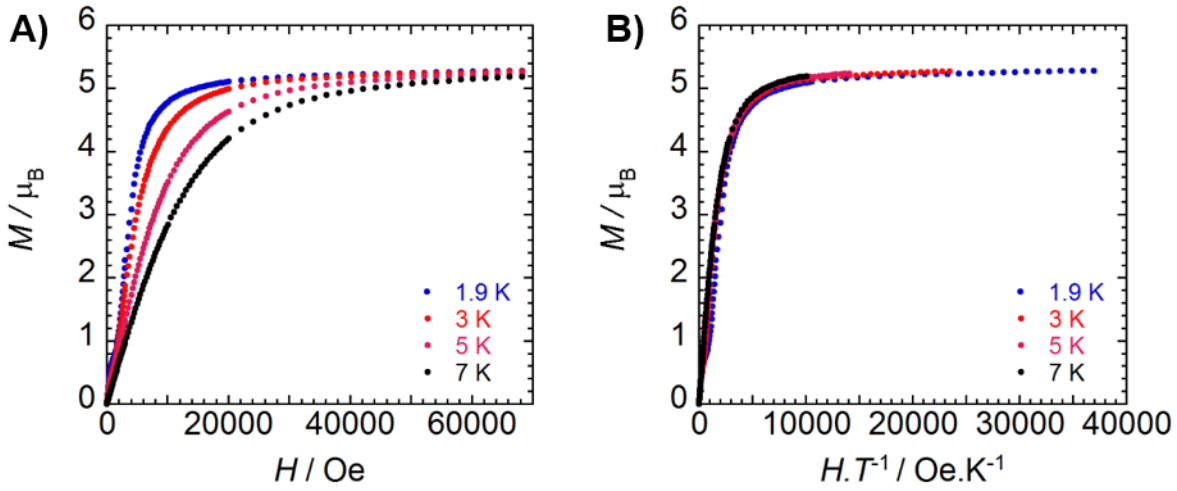

Figure S3. Field dependence of the (a) magnetization and (b) reduced magnetization for **1-Dy** at 1.9, 3, 5, and 7 K.

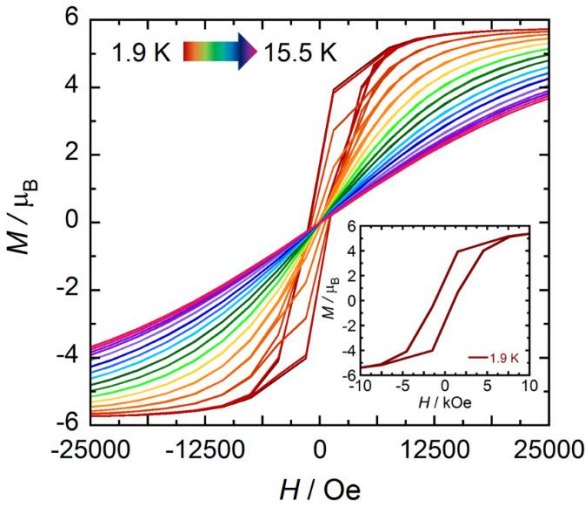

Figure S4. Magnetic hysteresis data for 1-Dy between 1.9 and 15.5 K. Data were collected at an average sweep rate of 23 Oe s^{-1}. In all measurements, data were collected starting at $H = 0$ Oe, sweeping to $H = 50$ kOe and then cycling to $H = -50$ kOe and back to $H = 50$ kOe. *Inset*: coercivity at 1.9 K.

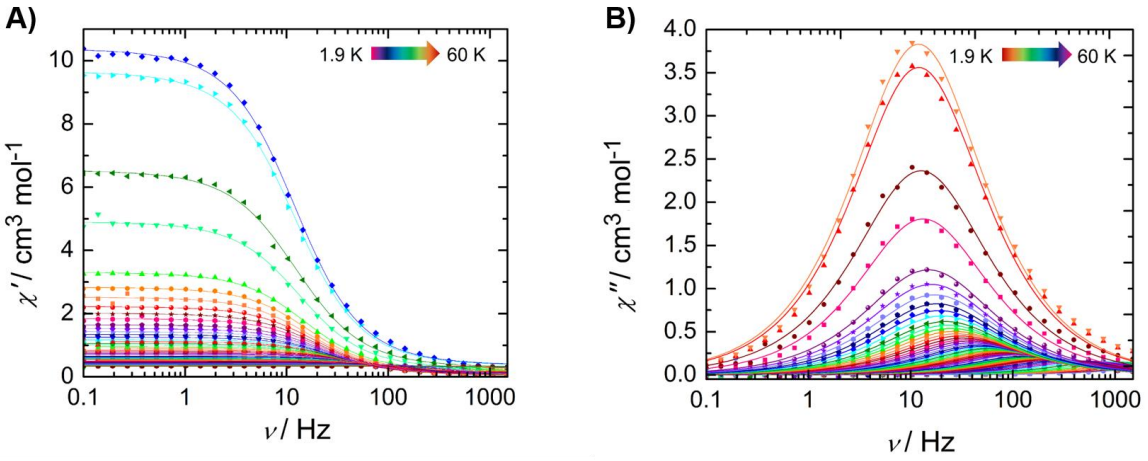

Figure S5. Frequency dependence of the zero field (a) in-phase and (b) out-of-phase magnetic susceptibility as a function of temperature for **1-Dy** between 1.9 and 60 K. Solid lines represent fits to the generalized Debye function, best fit parameters are found in Table S3 and S4 for in-phase and out-of-phase respectively.

Table S2. Fitting of the in-phase magnetic susceptibility plot to the generalized Debye model, values of α, χ_S, and χ_T for **1-Dy** under zero dc field at varying temperatures. Red values indicate when values were restrained to remain physically reasonable.

T (K)	τ (s)	α	χ_S	χ_T	χ_T- χ_S
1.9	0.013152	0.165216	0.366211	10.38233	10.01612
2	0.013121	0.165045	0.358165	9.666125	9.30796
3	0.012886	0.17141	0.296942	6.533747	6.236805
4	0.011896	0.156767	0.262871	4.905635	4.642764
6	0.01057	0.154055	0.200544	3.308393	3.10785
7	0.009864	0.146107	0.181818	2.833761	2.651942
8	0.009524	0.151405	0.162383	2.519807	2.357423
9	0.008727	0.144473	0.149905	2.226051	2.076146
10	0.008258	0.14449	0.137824	2.012243	1.874418
11	0.007773	0.138643	0.130312	1.844464	1.714151
12	0.007109	0.126775	0.122294	1.647037	1.524743
13	0.006732	0.128336	0.113023	1.529905	1.416882
14	0.006342	0.130127	0.104664	1.431636	1.326972
15	0.006002	0.130444	0.099084	1.343234	1.244151
16	0.005592	0.124258	0.095012	1.256748	1.161736
17	0.005181	0.110059	0.093214	1.175515	1.082301
18	0.004861	0.113619	0.08716	1.115419	1.028258
19	0.004506	0.107424	0.083381	1.055101	0.97172
20	0.004198	0.124215	0.074203	1.013588	0.939384
21	0.003938	0.105971	0.075853	0.955612	0.87976
22	0.003648	0.09938	0.074138	0.912614	0.838477
23	0.003404	0.093857	0.073576	0.872009	0.798434
24	0.003166	0.096764	0.06778	0.837122	0.769342
25	0.00297	0.089702	0.068547	0.802914	0.734367
26	0.002754	0.08596	0.065462	0.772291	0.706829
27	0.002575	0.087951	0.063068	0.744749	0.681681
28	0.002407	0.078773	0.063121	0.717901	0.654781
29	0.002242	0.077738	0.059015	0.69342	0.634406
30	0.002102	0.077044	0.058189	0.670522	0.612333
31	0.001954	0.07415	0.056234	0.649074	0.59284
32	0.001836	0.081162	0.0534	0.628972	0.575572
33	0.001717	0.070913	0.053673	0.609886	0.556213
34	0.001646	0.0634	0.056444	0.592296	0.535852
35	0.001511	0.049059	0.055338	0.568049	0.512711
36	0.001405	0.0442	0.055457	0.551741	0.496284
37	0.001339	0.081675	0.046474	0.547021	0.500547
38	0.001262	0.053985	0.050253	0.528405	0.478152
39	0.00117	0.056178	0.049113	0.512925	0.463811

40	0.001129	0.057111	0.050195	0.504258	0.454063
41	0.001039	0.062829	0.044747	0.492398	0.447651
42	9.84E-04	0.054557	0.047273	0.480339	0.433066
43	9.08E-04	0.05559	0.046521	0.468943	0.422422
44	8.84E-04	-9.05E-19	0.060962	0.455022	0.39406
45	7.69E-04	0.045319	0.047365	0.448159	0.400794
46	7.01E-04	0.049128	0.046595	0.438711	0.392116
47	6.16E-04	0.05441	0.046082	0.430984	0.384902
48	5.31E-04	0.062579	0.04176	0.42146	0.3797
49	4.77E-04	0.046002	0.057115	0.412045	0.35493
50	4.26E-04	8.57E-20	0.072603	0.40266	0.330057
51	3.44E-04	8.00E-20	0.072897	0.395111	0.322214
52	2.51E-04	0.055207	0.055203	0.389142	0.333939
53	1.98E-04	0.05836	0.059657	0.382082	0.322425
54	1.46E-04	0.066836	0.044362	0.375302	0.33094
55	1.38E-04	0.036311	0.103092	0.368674	0.265581
56	9.13E-05	0.063519	0.068095	0.362739	0.294645
57	5.45E-05	0.07962	0	0.35636	0.35636
58	6.11E-05	0.046574	0.11558	0.350092	0.234512
59	3.51E-05	0.03752	0.01102	0.343497	0.332477
60	2.31E-05	0.057928	0	0.337497	0.337497

Table S3. Fitting of the out-of-phase magnetic susceptibility plot to the generalized Debye model, values of α, χ_S, and χ_T for **1-Dy** under zero dc field at varying temperatures. Red values indicate when values were restrained to remain physically reasonable.

T (K)	τ (s)	α	χ_S	χ_T	χ_T- χ_S
1.9	0.013335	0.167723	0.68702	10.69033	10.00331
2	0.01327	0.167519	0.618414	9.913056	9.294643
3	0.012585	0.171544	0.207183	6.419566	6.212383
4	0.012016	0.159691	0.152493	4.808619	4.656127
6	0.010633	0.154795	0.504493	3.617582	3.113089
7	0.01	0.152179	0.454889	3.1236	2.668711
8	0.009289	0.153483	0.418397	2.785169	2.366773
9	0.008822	0.147771	0.366762	2.450516	2.083754
10	0.008303	0.14521	0.315393	2.192371	1.876978
11	0.007769	0.141967	0.273023	1.982883	1.70986
12	0.007208	0.136658	1.050578	2.587287	1.536709
13	0.006819	0.134108	0.200884	1.626404	1.42552
14	0.00639	0.136617	0.197463	1.534161	1.336698
15	0.006008	0.13474	0.195462	1.445423	1.249962
16	0.005587	0.128148	0.188146	1.356067	1.167922
17	0.005239	0.122674	0.183001	1.278336	1.095336
18	0.004867	0.128505	0.190125	1.235501	1.045376
19	0.004512	0.116016	0.190114	1.17187	0.981756
20	0.004206	0.107102	0.116815	1.046078	0.929263
21	0.003918	0.110856	0.106541	0.996252	0.889711
22	0.003635	0.104179	0.125793	0.970338	0.844545
23	0.003414	0.102956	0.13009	0.938398	0.808307
24	0.003168	0.100537	0.134941	0.911015	0.776075
25	0.002946	0.101866	0.171162	0.916497	0.745335
26	0.002736	0.09837	0.136596	0.853765	0.717169
27	0.002578	0.089724	0.139117	0.827279	0.688162
28	0.002384	0.091222	0.141814	0.802321	0.660507
29	0.002225	0.09072	0.151453	0.791733	0.64028
30	0.002075	0.088964	0.175416	0.793771	0.618354
31	0.001946	0.082649	0.1503	0.752061	0.601761
32	0.001819	0.084527	0.211174	0.793317	0.582142
33	0.001718	0.077888	0.212769	0.773369	0.5606
34	0.001607	0.0745	0.219586	0.764345	0.544759
35	0.001484	0.05268	0.228104	0.744344	0.51624
36	0.001427	0.079364	0.236796	0.752568	0.515771
37	0.001245	0.074435	0.002714	0.488391	0.485677
38	0.001251	0.082944	0.039116	0.530494	0.491378
39	0.001188	0.067359	1.28E-04	0.475278	0.47515

40	0.001106	0.072317	0.003659	0.466886	0.463227
41	0.00104	0.069685	3.91E-04	0.452265	0.451875
42	9.61E-04	0.073823	1.43E-04	0.443963	0.44382
43	8.90E-04	0.073428	7.83E-04	0.432333	0.43155
44	8.29E-04	0.069157	0.002932	0.422462	0.41953
45	7.62E-04	0.068625	0.00388	0.413583	0.409704
46	6.83E-04	0.069928	0.002712	0.404859	0.402147
47	6.09E-04	0.062393	0.002255	0.395553	0.393298
48	5.26E-04	0.078073	3.17E-04	0.388724	0.388408
49	4.46E-04	0.075358	0.002727	0.380423	0.377696
50	3.69E-04	0.072931	3.58E-05	0.367405	0.367369
51	3.05E-04	0.073401	0.003187	0.362272	0.359086
52	2.41E-04	0.080663	8.91E-04	0.354785	0.353894
53	1.94E-04	0.062843	0.040329	0.37392	0.33359
54	1.51E-04	0.057295	0.010844	0.338157	0.327313
55	1.16E-04	0.048512	9.55E-04	0.315838	0.314883
56	7.70E-05	0.075815	0	0.335157	0.335157
57	7.74E-05	0.029958	0	0.277406	0.277406
58	5.50E-05	0.042165	0.002559	0.289496	0.286937
59	2.75E-05	0.100021	0	0.362225	0.362225
60	1.09E-05	0.112438	0	0.626048	0.626048

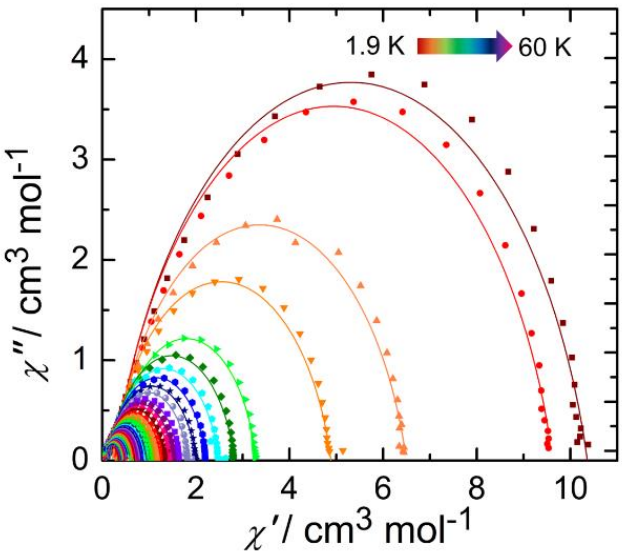

Figure S6. Cole-Cole (Argand) plot for ac susceptibility of **1-Dy** collected under 0 Oe dc field between 1.9 and 60 K. Solid lines represent the fit to generalized Debye function. The best fit parameters are provided in Table S4.

Table S4. Fitting of Cole-Cole plots, values of α, χ_S, and χ_T for **1-Dy** under zero dc field at varying temperatures. Red values indicate when values were restrained to remain physically reasonable.

T (K)	τ (s)	α	χ_S	χ_T
1.9	0.01017943	0.22444	1.22011	9.40106
2	0.01028223	0.21473	1.11900	8.77143
3	0.01002806	0.21992	0.81799	5.91215
4	0.00957434	0.20462	0.61983	4.47657
6	0.00527960	0.50000	0.14254	3.09043
7	0.00628629	0.36233	0.36233	2.61287
8	0.00770544	0.18729	0.32968	2.30254
9	0.00722238	0.17251	0.28755	2.05964
10	0.00679280	0.17772	0.26612	1.85988
11	0.00644486	0.17120	0.24139	1.70243
12	0.00585467	0.17708	0.22174	1.52656
13	0.00554290	0.17744	0.20584	1.41877
14	0.00540359	0.14920	0.18096	1.33838
15	0.00514013	0.14515	0.16916	1.25344
16	0.00482519	0.13871	0.15707	1.17810
17	0.00443438	0.14541	0.15089	1.10446
18	0.00420544	0.13615	0.13948	1.04869
19	0.00398691	0.11709	0.12681	1.00012
20	0.00373197	0.11435	0.12142	0.95251
21	0.00341864	0.10877	0.11342	0.90836
22	0.00338136	0.10512	0.10786	0.86930
23	0.00302958	0.09338	0.10538	0.83510
24	0.00283731	0.10666	0.09940	0.79781
25	0.00268958	0.09664	0.09481	0.76823
26	0.00248701	0.09930	0.09106	0.73879
27	0.00235649	0.08782	0.08581	0.71490
28	0.00218877	0.09315	0.08500	0.68898
29	0.00205621	0.08564	0.07936	0.66711
30	0.00198512	0.05826	0.07637	0.65147
31	0.00182335	0.06980	0.07240	0.62836
32	0.00168432	0.08599	0.07232	0.60510
33	0.00157254	0.08656	0.06982	0.58690
34	0.00154029	0.06699	0.06980	0.57472
35	0.00134597	0.12178	0.07231	0.56074
36	0.00131925	0.07516	0.06668	0.54347
37	0.00121445	0.10018	0.06671	0.52905
38	0.00114975	0.09622	0.06274	0.51573
39	0.00108922	0.08258	0.06097	0.50232
40	0.00104989	0.07249	0.05999	0.48858
41	0.00097630	0.06247	0.05539	0.47845
42	0.00091192	0.07566	0.05549	0.46491

43	0.00083320	0.08332	0.05534	0.08332
44	0.00079753	0.05953	0.05537	0.44681
45	0.00075102	0.02401	0.05232	0.44029
46	0.00068329	0.02521	0.05100	0.43141
47	0.00058564	0.04679	0.05228	0.42132
48	0.00050465	0.04881	0.05057	0.41166
49	0.00045342	0.04634	0.05667	0.40314
50	0.00036067	0.07240	0.05288	0.39215
51	0.00029360	0.06790	0.05289	0.38571
52	0.00023944	0.02671	0.06249	0.38414
53	0.00018777	0.01930	0.07004	0.37645
54	0.00013239	0.00658	0.07419	0.37242
55	0.00012145	0.06178	0.05678	0.35861
56	6.8699E-05	0.13999	0	0.33834
57	4.2751E-07	0.13984	0	0.33285
58	4.7524E-08	0.19154	0	0.31075

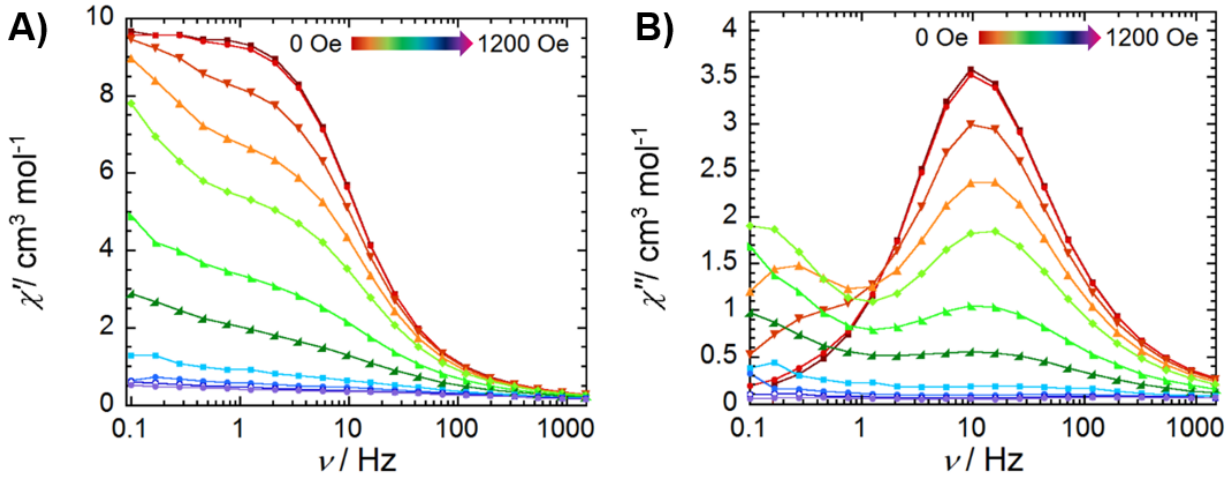

Figure S7. Frequency dependence of (a) the in-phase and (b) the out-of-phase magnetic susceptibility as a function of the applied field for **1-Dy**.

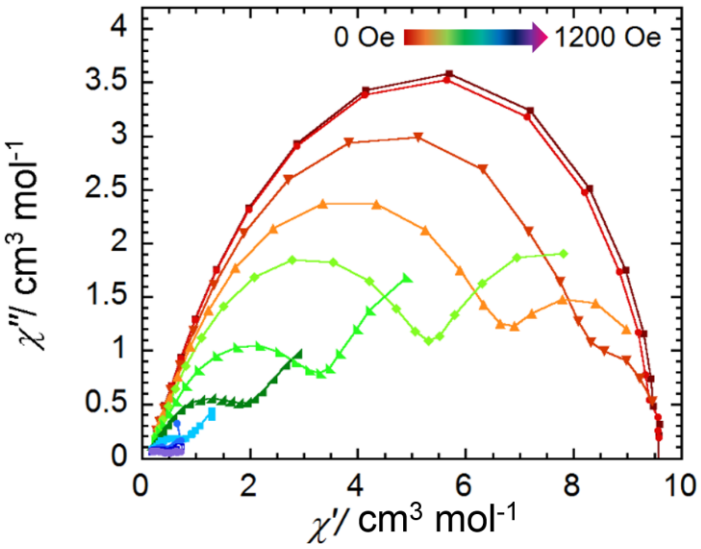

Figure S8. Cole-Cole (Argand) plots for the determination of the field dependence of τ for **1-Dy** at 2 K. Solid lines are guides for the eye. The best fit parameters for the data are provided in Table S2.

Table S5. Fitting of Cole-Cole plots, values of τ, α, χ_S, and χ_T for **1-Dy** at 2 K, varying applied dc fields for the determination of the field dependence of τ for **1-Dy** at 2 K. The values pertain to the primary relaxation process, the secondary process could not be fit with physically reasonable values. Values collected above 600 Oe did not yield physically reasonable values and were not considered.

H (Oe)	τ (s)	α	χ_S	χ_T
0	0.00984749	0.24896	1.24964	8.85874
50	0.01004122	0.23505	1.18501	8.73438
100	0.00889019	0.31123	1.32418	7.73946
150	0.00761567	0.36541	1.28610	6.37279
200	0.00666255	0.42602	1.21936	5.06447
300	0.00472470	0.63618	1.23705	2.99020
400	0.01099896	0.86949	1.11397	1.51162
600	18736200.9	0.88769	0.5791	0.46413
800	-	-	-	-
1000	-	-	-	-
1200	-	-	-	-

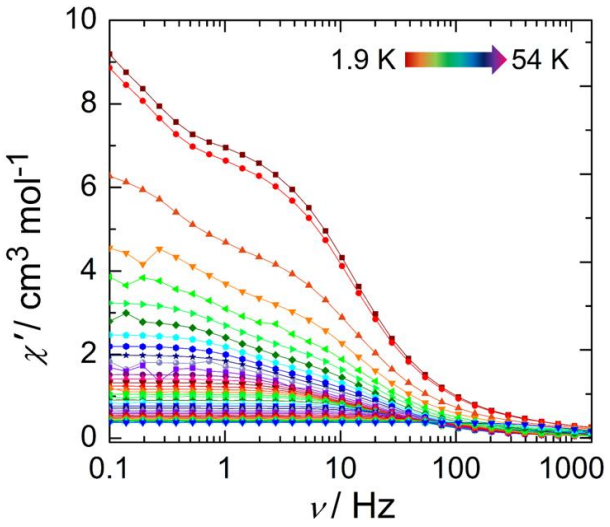

Figure S9. Frequency dependence of the in-phase magnetic susceptibility as a function of temperature for **1-Dy** between 1.9 and 54 K, collected under an applied dc field of 150 Oe. Solid lines are guides for the eye.

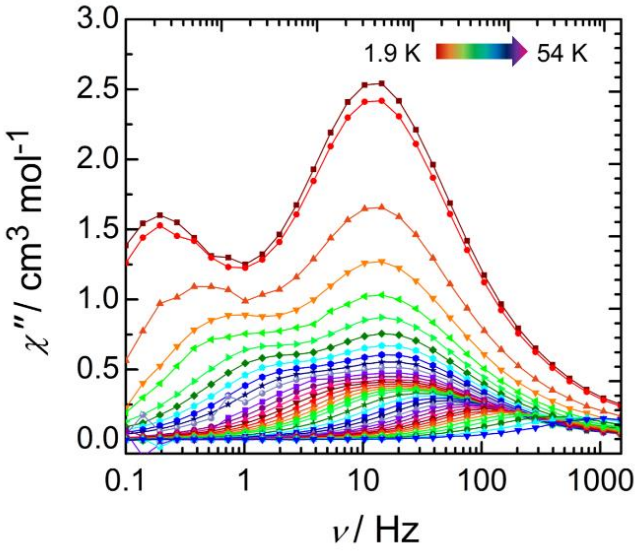

Figure S10. Frequency dependence of the out-of-phase (χ'') component of the ac magnetic susceptibility for 1-Dy under 150 Oe applied dc field from 1.9 K to 54 K. Solid lines are guides for the eye.

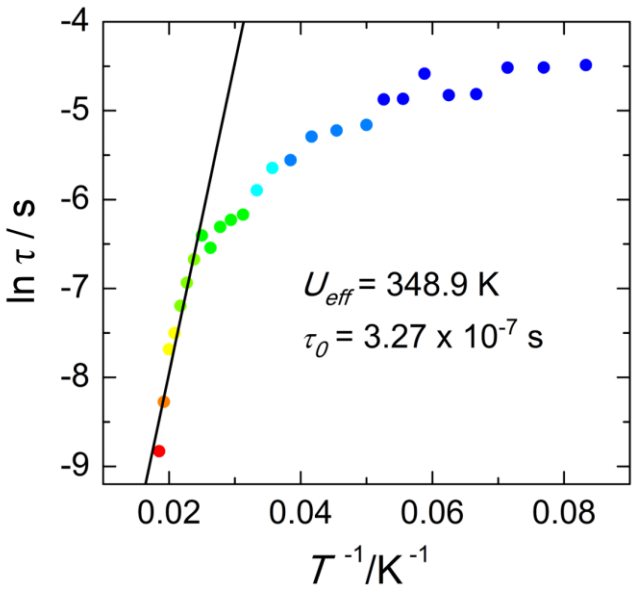

Figure S11. Relaxation time of the magnetization, *ln(τ) vs.* T^{-1} for **1-Dy** (Arrhenius plot using ac data) under 150 Oe applied dc field. The solid black line corresponds to the fit.

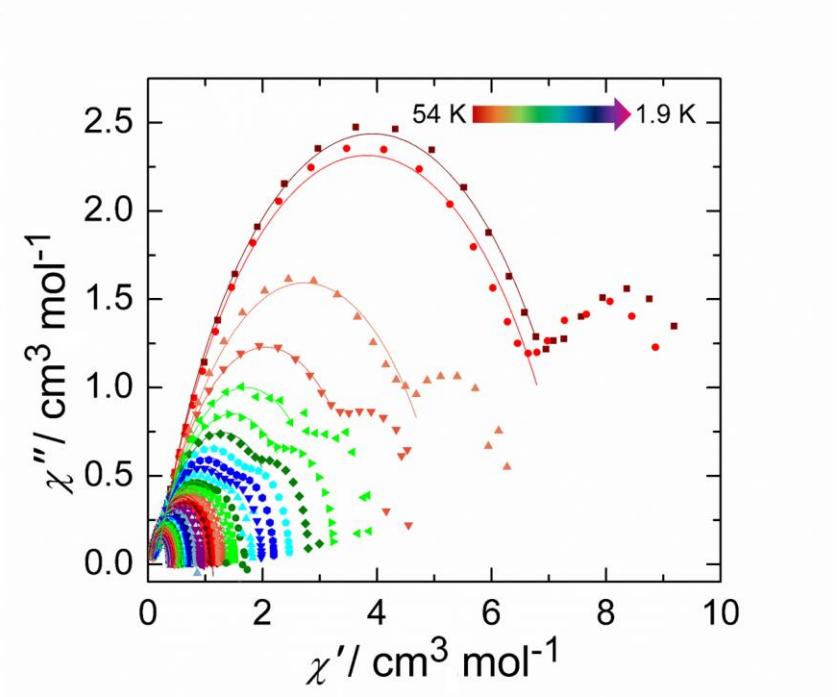

Figure S12. Cole-Cole (Argand) plot for ac susceptibility of **1-Dy** collected under 150 Oe between 1.9 and 54 K. Solid lines represent the fit for the primary relaxation processes to generalized Debye function. The secondary process could not be fit with physically reasonable values. The best fit parameters are provided in Table S6.

Table S6. Fitting of Cole-Cole plots, values of τ, α, χ_S, and χ_T for **1-Dy** under zero dc field at varying temperatures. The values pertain to the primary relaxation process, the secondary process could not be fit with physically reasonable values. Above 12 K, the relaxation processes could not be determined to be independent of one another, as such the isotemperature curves were fit as a single relaxation process.

T (K)	τ (s)	α	χ_S	χ_T
1.9	0.01145942	0.35781	1.29208	6.54839
2	0.01144594	0.38914	1.34586	6.29130
3	0.01422262	0.41550	1.04949	4.41542
4	0.01652162	0.36348	0.73760	3.38350
5	0.01330554	0.37724	0.63419	2.78037
6	0.01264193	0.38923	0.56245	2.37920
7	0.01257694	0.39016	0.50254	2.09535
8	0.01137214	0.35149	0.41075	1.83673
9	0.00979008	0.38426	0.40397	1.69293
10	0.00877107	0.39363	0.38190	1.56573
11	0.00763191	0.40394	0.36476	1.46577
12	0.00676672	0.40421	0.33806	1.35678
13	0.00649030	0.39329	0.31759	1.31254
14	0.00629522	0.35553	0.27819	1.24146
15	0.00605786	0.32259	0.24673	1.17584
16	0.00573529	0.29277	0.22016	1.11516
17	0.00535401	0.27221	0.19905	1.05776
18	0.00514384	0.24894	0.18111	1.00897
19	0.00475695	0.22433	0.16360	0.96386
20	0.00426052	0.22556	0.15560	0.91321
22	0.00378991	0.18762	0.13322	0.84595
24	0.00331184	0.15340	0.11308	0.78456
26	0.00284169	0.13295	0.10105	0.72980
28	0.00239066	0.14066	0.09400	0.67765
30	0.00214486	0.10874	0.08280	0.64015
32	0.00182772	0.10736	0.07822	0.60110
34	0.00162590	0.08811	0.07052	0.57000
36	0.00143152	0.08247	0.06576	0.53982
38	0.00126681	0.07310	0.06342	0.51338
40	0.00111814	0.06755	0.06016	0.48899
42	0.00137375	0.03511	0.05240	0.47225
44	0.00082416	0.06324	0.05460	0.44624
46	0.00068542	0.06848	0.05320	0.42620
48	0.00048020	0.13353	0.05031	0.39974
50	0.00035659	0.08986	0.04952	0.38989
52	0.00024377	0.04589	0.05894	0.38131
54	0.00016003	0.01142	0.07623	0.37097

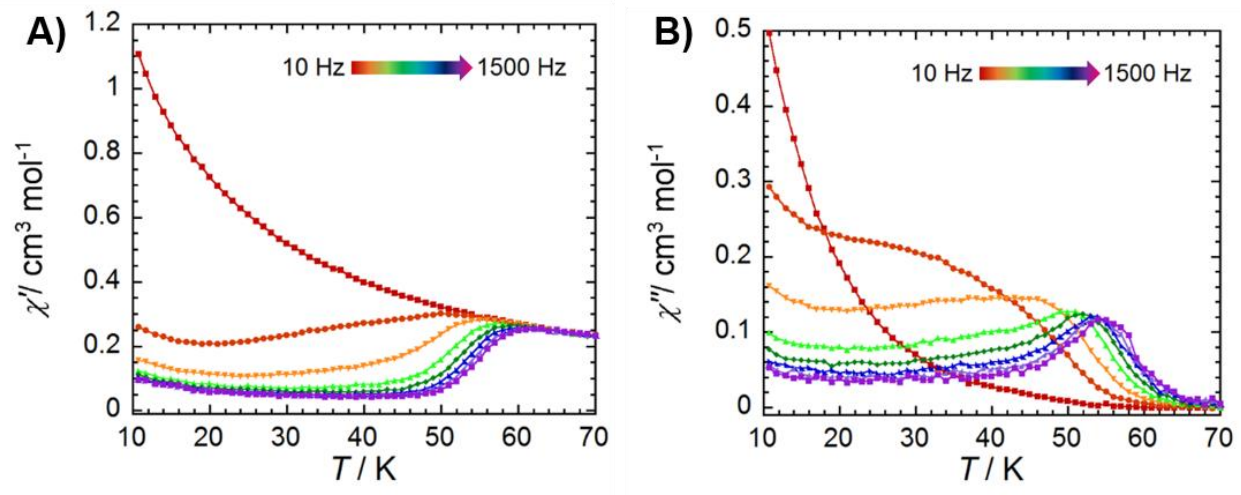

Figure S13. Temperature dependence of (a) the in-phase and (b) the out-of-phase magnetic susceptibility as a function of frequency for **1-Dy**, under zero applied dc field.

Details of the *Ab Initio* Calculations

All calculations were of the CASSCF/RASSI/SINGLE_ANISO kind using the MOLCAS-8.0 program package.[1] All atoms were described using all electron relativistic ANO-RCC basis sets.[2] Basis set contractions are given in Table S7. Standard complete active space self-consistent field (CASSCF) calculations on the full molecular structure were performed.[3] In these calculations, the $4f^9$ electronic shell of the Dy^{III} is explicitly correlated, i.e., the active space, while the remaining orbitals are described in the mean field approach (as in the conventional Hartree-Fock SCF model). All possible electronic states (of various total spins) arising from the chosen active space were optimized self-consistently and a subset of them was further mixed by the spin-orbit coupling (RASSI).[4]

Table S7. Contractions of the employed basis sets describing each of the atom in the investigated molecules.

Atom	Basis set contraction	
Dy	8s7p5d3f2g1h	ANO-RCC-VTZP.
I	7s6p4d2f1g	ANO-RCC-VTZP.
Fe	6s5p3d2f1g	ANO-RCC-VTZP
Si	5s4p2d1f	ANO-RCC-VTZP
O	4s3p2d1f	ANO-RCC-VTZP
N	4s3p2d1f	ANO-RCC-VTZP
C (close)	4s3p2d1f	ANO-RCC-VTZP
C (distant)	3s2p1d	ANO-RCC-VDZP
H	2s1p	ANO-RCC-VDZP

Relativistic effects were considered in two steps, both based on Douglas Kroll Hess Hamiltonian. Scalar relativistic effects are included in the basis sets describing each atom (Table S7). All mono and bielectronic integrals (Couloumb, Exchange, angular momentum, AMFI, etc.) in this basis are computed and used in the subsequent calculations. Complete active space self consistent-field calculations were carried out using the $4f^9$ shell of the Dy^{3+} site as active space. All possible electronic states arising from the active space were calculated in the mean field of other electrons. 21 spin sextet, 128 spin quartet and 130 spin doublet states were admixed by the spin-orbit coupling in the RASSI method. The spin orbit coupling was accounted within Atomic Mean Field approximation (AMFI). On the basis of the resulting spin-orbit states, all magnetic properties were computed within the SINGLE_ANISO program in MOLCAS 8.0. The parameters of the effective crystal-field Hamiltonian were extracted and are displayed in Table S9.

Table S8. Energy splitting of the ground free ion J = 15/2 multiplet in various computational models (cm-1) and magnetic anisotropy in the lowest three Kramers doublet states.

KD		**1-Dy**	**1-noTHF**	**1-noI**	**1-noTHFnoI**
1		**0.0**	**0.0**	**0.0**	**0.0**
2		**414.6**	**492.5**	**488.8**	**622.2**
3		**692.2**	**890.3**	**802.0**	**1166.5**
4		803.0	1176.9	921.4	**1591.1**
5		903.3	1359.1	1111.5	1874.0
6		1038.8	1557.3	1364.1	2025.3
7		1197.7	1804.6	1653.0	2112.5
8		1327.8	2030.6	1911.8	2213.4
		g tensors in the low-lying Kramers doublet states			
	g_X	4.4×10^{-4}	2.4×10^{-5}	4.3×10^{-4}	3.2×10^{-8}
1	g_Y	4.9×10^{-4}	3.0×10^{-5}	5.6×10^{-4}	1.6×10^{-7}
	g_Z	19.8894	19.8986	19.9113	19.9677
	g_X	0.0066	2.0×10^{-3}	0.0412	2.5×10^{-5}
2	g_Y	0.0104	2.6×10^{-3}	0.0651	2.6×10^{-5}
	g_Z	16.9721	16.8893	16.7914	17.0067
	g_X	0.8911	0.1210	2.2968	0.0010
3	g_Y	1.7114	0.1662	6.0679	0.0011
	g_Z	13.2157	13.7224	10.5290	14.1568
	g_X	3.8174	2.0871	7.2834	0.0328
4	g_Y	5.0097	3.0000	6.0380	0.0350
	g_Z	11.4701	9.7303	1.5554	11.4146

Table S9. Parameters of the crystal field acting of the ground *J*=15/2 multiplet for all investigated structures, corresponding to the *ab initio* calculations described above. Quantisation axis is chosen the main anisotropy axis in the ground Kramers doublet state (approx. N1-N2 direction).

Rank	**Proj.**	**1-Dy**	**1-noTHF**	**1-noI**	**1-noTHFnoI**
	-2	**-0.400645E+01**	0.101038E+00	**-0.106631E+01**	**-0.161376E+01**
	-1	0.405941E+00	-0.466676E+00	-0.184903E-01	0.440251E-01
2	0	**-0.647155E+01**	**-0.103589E+02**	**-0.862108E+01**	**-0.129657E+02**
	1	-0.258180E+00	0.129652E+00	-0.993762E-01	0.351901E-01
	2	-0.536278E+00	**0.716930E+01**	**0.891364E+01**	**0.156931E+01**
	-4	-0.176839E-01	-0.314061E-02	0.872897E-02	-0.232835E-03
	-3	0.182484E-02	0.166613E-02	-0.553989E-03	-0.650243E-03
	-2	0.161532E-01	-0.580665E-02	0.103611E-01	-0.649060E-02
	-1	-0.218958E-02	0.321342E-02	-0.140399E-03	0.318659E-03
4	0	-0.740658E-02	-0.552651E-02	-0.845928E-02	**-0.719447E-02**
	1	0.205642E-02	-0.129581E-02	0.244054E-03	-0.388185E-03
	2	0.129277E-01	0.234839E-02	-0.195618E-01	-0.138344E-02
	3	0.245634E-02	-0.238604E-02	-0.200580E-04	-0.531144E-03
	4	0.194404E-01	-0.373949E-02	-0.190455E-01	-0.196106E-02
	-6	-0.660711E-04	-0.319114E-04	0.149223E-03	-0.196025E-05
	-5	0.769051E-04	0.530290E-04	-0.270091E-04	0.492283E-05
	-4	-0.737630E-04	-0.479799E-04	0.303649E-04	0.764432E-05
	-3	0.838110E-05	0.359969E-04	-0.581991E-05	-0.501807E-06
	-2	-0.830042E-05	0.320602E-04	-0.677317E-04	**0.105020E-03**
	-1	-0.114537E-04	0.627986E-05	0.478879E-05	0.452025E-06
6	0	0.487678E-05	0.208189E-04	0.165015E-04	0.335544E-04
	1	-0.364130E-05	0.793350E-05	-0.218247E-06	0.463353E-05
	2	-0.671008E-04	-0.152339E-03	-0.408894E-04	-0.311725E-04
	3	0.394618E-04	-0.226759E-05	0.536208E-05	0.982786E-05
	4	0.151552E-03	-0.223556E-04	-0.156674E-03	-0.344556E-04
	5	-0.112542E-04	-0.501193E-04	-0.626646E-05	0.332071E-05
	6	-0.155335E-03	-0.267344E-04	-0.142060E-03	-0.113796E-04
		Recovery factor of the initial ab initio CF matrix*			
		99.2%	99.0%	99.3%	99.0%

* The recovery factor shows the amount of the initial CF matrix which is reproduced by the above shown CF parameters, in %. The cumulative effect of the non-CF parameters (ranks 8,10,12, 14) is (100%-recovery_factor), i.e., less than 1% for all cases.

Analysis of the relaxation rates *via* different excited states

At a first glance, the matrix element connecting the opposite components of the KD3 is sufficiently large (0.45 μ_B) to suggest that this doublet is the top of the barrier (see Figure 3 in the main text). However, this matrix element is much larger (2.9 μ_B) for the KD4, so that tunneling through the barrier can take place at this doublet for a sufficiently high temperature. Indeed, the rate of thermally assisted tunneling transition (TAT) is the product of the Boltzmann population of a given doublet and the rate of incoherent tunneling transition between the components with opposite magnetization.[5] Because the latter is roughly proportional to the square of the magnetic moment, μ, of the corresponding doublet state,[6] the rate of TAT is proportional to $\sim\mu^2 e^{-\frac{E}{kT}}$, where E is the energy of the doublet and k is the Boltzmann constant. Using the data from Table S8 and Figure 3, the temperature dependence of this function is plotted below (Figure S14). At T = 52 K, the ratio between relaxation *via* KD4 and KD3 ≈ 2, while this ratio doubles its value already at T = 70 K.

This ratio shows an increase with temperature (see Figures S14 and S15), implying that the activated relaxation *via* the KD4 becomes dominant in the temperature domain where a linear $ln(\tau) = f\left(\frac{1}{T}\right)$ dependence is observed.

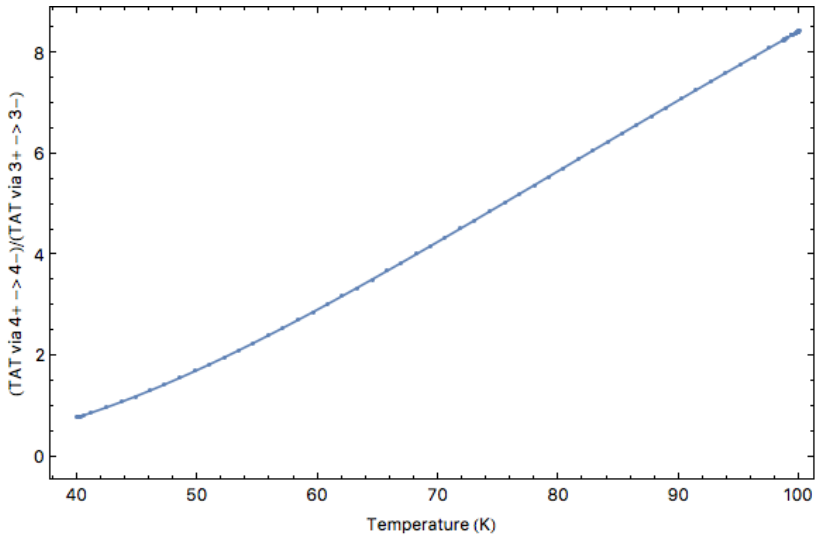

Figure S14. Temperature dependence of the ratio between TAT rates in the KD4 and KD3.

As a comparison, the ratio between TAT rates in the KD3 and KD2 is plotted below. The steep rise of the ratio with temperature shows that the TAT relaxation *via* KD2 is almost negligible in this temperature domain.

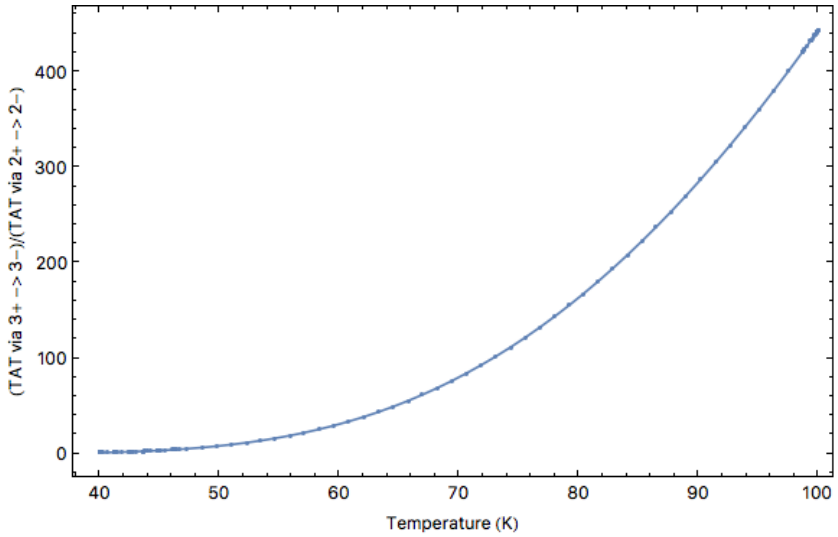

Figure S15. Temperature dependence of the ratio between TAT rates in the KD3 and KD2.

References

1. Aquilante, F.; Autschbach, J.; Carlson, R. K.; Chibotaru, L. F.; Delcey, M. G.; De Vico, L.; Galvan, I. F.; Ferre, N.; Frutos, L. M.; Gagliardi, L.; Garavelli, M.; Giussani, A.; Hoyer, C. E.; Li Manni, G.; Lischka, H.; Ma, D.; Malmqvist, P. A.; Mueller, T.; Nenov, A.; Olivucci, M.; Pedersen, T. B.; Peng, D.; Plasser, F.; Pritchard, B.; Reiher, M.; Rivalta, I.; Schapiro, I.; Segarra-Marti, J.; Stenrup, M.; Truhlar, D. G.; Ungur, L.; Valentini, A.; Vancoillie, S.; Veryazov, V.; Vysotskiy, V. P.; Weingart, O.; Zapata, F.; Lindh, R. *J. Comput. Chem.* **2016,** *37*, 506-541.
2. Roos, B. O.; Lindh, R.; Malmqvist, P.-A.; Veryazov, V.; Widmark, P.-O.; Borin, A. C. *J. Phys. Chem. A* **2008,** *112*, 11431-11435.
3. Roos, B. O., In *Advances in Chemical Physics; Ab Initio Methods in Quantum Chemistry - II*, Lawley, K. P., Ed. Wiley: Chichester, 1987; p 399.
4. Malmqvist, P. A.; Roos, B. O.; Schimmelpfennig, B. *Chem. Phys. Lett.* **2002,** *357*, 230-240
5. Garanin, D. A.; Chudnovsky, E. M. *Phys. Rev. B: Condens. Matter Mater. Phys*. **1997**, *56*, 11102.
6. Ungur, L.; Thewissen, M.; Costes, J.-P.; Wernsdorfer, W.; Chibotaru, L. F. *Inorg. Chem.* **2013**, *52*, 6328.